Atmos. Chem. Phys. Discuss., https://doi.org/10.5194/acp-2018-640
Manuscript under review for journal Atmos. Chem. Phys.
Discussion started: 7 September 2018

Atmospheric Chemistry and Physics Discussions

Transport of short-lived halocarbons to the stratosphere over the Pacific Ocean.

Michal T. Filus[1], Elliot L. Atlas[2], Maria A. Navarro[2*], Elena Meneguz[3], David Thomson[3], Matthew J. Ashfold[4], Lucy J. Carpenter[5], Stephen J. Andrews[5], Neil R.P. Harris[6]

1. Centre for Atmospheric Science, University of Cambridge, Cambridge, CB2 1EW, UK
2. Department of Atmospheric Sciences, RSMAS, University of Miami, Miami, Florida, USA
3. Met Office, Atmospheric Dispersion Group, FitzRoy Road, Exeter, EX1 3PB, UK
4. School of Environmental and Geographical Sciences, University of Nottingham Malaysia Campus, 43500,Semenyih, Selangor, Malaysia
5. Wolfson Atmospheric Chemistry Laboratories, Department of Chemistry, University of York, York, YO10 5DD, UK
6. Centre for Environmental and Agricultural Informatics, Cranfield University, Cranfield, MK43 0AL, UK

Correspondence to: Neil Harris (neil.harris@cranfield.ac.uk)

Abstract. The effectiveness of transport of short-lived halocarbons to the upper troposphere and lower stratosphere remains an important unknown in quantifying the supply of ozone-depleting substances to the stratosphere. In early 2014, a major field campaign in Guam in the West Pacific, involving UK and US research aircraft, sampled the tropical troposphere and lower stratosphere. The resulting measurements of CH_3I, $CHBr_3$ and CH_2Br_2 are compared here with calculations from a Lagrangian model. This methodology benefits from an updated convection scheme which improves simulation of the effect of deep convective motions on particle distribution within the tropical troposphere. We find that the observed CH_3I, $CHBr_3$ and CH_2Br_2 mixing ratios in the Tropical Tropopause Layer (TTL) are consistent with those in the boundary layer when the new convection scheme is used to account for convective transport. Particularly, comparisons between modelled estimates and observations of shortest-lived CH_3I indicates that the NAME convection scheme is realistic up to the lower TTL but less good at reproducing the small number of extreme convective events in the upper TTL. This study consolidates our understanding of the transport of short-lived halocarbons to the upper troposphere and lower stratosphere by using improved model calculations to confirm consistency between observations in the boundary layer, observations in the TTL, and atmospheric transport processes. Our results support recent estimates of the contribution of short-lived bromocarbons to the stratospheric bromine budget.

1 Introduction

The successful implementation of the Montreal Protocol with its adjustments and amendments has led to reductions in stratospheric chlorine and bromine amounts since the late 1990s (Carpenter et al., 2014). These reductions have halted the ozone decrease (Harris et al., 2015; Chipperfield et al., 2017; Steinbrecht et al., 2017) with the exception of continued depletion in the lower stratosphere (Ball et al., 2017). Recently, the importance of very short-lived (VSL) chlorine- and bromine containing

*Deceased: 19.12.2017

compounds has received a great deal of attention (e.g. Hossaini et al., 2017; Oram et al., 2017). VSLS are not considered under the Montreal Protocol, but are required in order to ensure reconcile between observed stratospheric measurements of inorganic or 'active' bromine with reported anthropogenic bromine emission sources. VSLS input into the stratosphere has however remained a poorly constrained quantity (Carpenter et al., 2014), which hinders our understanding of the on-going decline in lower stratospheric ozone and our ability to make predictions of stratospheric ozone recovery.

Three of the most important VSL halocarbons are CH_3I, $CHBr_3$ and CH_2Br_2. They have typical lower tropospheric lifetimes (4, 15 and 94 days, respectively (Carpenter et al., 2014)) which are shorter than tropospheric transport timescales and so they have non-uniform tropospheric abundances. They are all emitted predominantly from the oceans and result principally from natural sources (e.g. Lovelock 1975; Solomon et al., 1994; Oram and Penkett, 1994; Vogt et al., 1999; Salawitch et al., 2006; Pyle et al., 2011; Carpenter et al., 2012, 2014; Tegtmeier et al., 2013; Saiz-Lopez et al., 2014). The short-lived bromocarbons, chiefly $CHBr_3$ and CH_2Br_2, have been identified as the missing source for the stratospheric active bromine (mostly originating from long-lived brominated organic and inorganic substances; Pfeilsticker et al., 2000; Salawitch, 2006; Feng et al., 2007; Dessens et al., 2009). The current estimates of the contribution of the short-lived bromocarbons to the active bromine (Br_y) in the stratosphere range from 3-8 ppt (Liang et al., 2010, 2014; Carpenter et al., 2014; Fernandez et al., 2014; Sala et al., 2014; Tegtmeier et al., 2015; Navarro et al., 2015, 2017; Hossaini et al., 2016; Butler et al., 2017; Fiehn et al., 2017). Much of this uncertainty is linked to the contribution of $CHBr_3$ which has both the shortest lifetime and the largest emissions of the commonly observed bromocarbons.

The transport of VSL halocarbons into the lower stratosphere is by ascent through the tropical tropopause layer (TTL) (Fueglistaler et al., 2009). An important factor influencing the loading of the VSL bromocarbons in the TTL is the strength of the convective transport from the boundary layer where the bromocarbons are emitted (Hosking et al., 2010; Russo et al., 2015; Fuhlbrügge et al., 2016; Krzysztofiak et al., 2018). This is poorly quantified and, especially when taken together with the large variations in boundary layer concentrations and the convection parameterisation being the major source of uncertainty in chemistry transport models, limits our ability to model the bromine budget in the current and future atmosphere (Liang et al., 2010, 2014; Hoyle et al., 2011; Russo et al., 2011, 2015; Schofield et al., 2011; Aschmann et al., 2013; Fernandez et al., 2014; Hossaini et al., 2016; Krzysztofiak et al., 2018).

To address this and other challenges, the Natural Environment Research Council Coordinated Airborne Studies in the Tropics (NERC CAST), National Centre for Atmospheric Research Convective Transport of Active Species in the Tropics (NCAR CONTRAST) and National Aeronautics and Space Administration Airborne Tropical Tropopause Experiment (NASA ATTREX) projects were organised (Harris et al., 2017; Jensen et al., 2017; Pan et al., 2017). These projects joined forces in January-March 2014 in the American territory of Guam, in the West Pacific. Three aircraft were deployed to sample air masses at different altitudes to investigate the

characteristics of the air masses affected by the deep convective systems. This campaign produced a unique dataset of coordinated measurements for interpretative studies of transport and distribution of the chemical species, including the VSL bromocarbons (Sect. 2.1 and 2.2). The NASA ATTREX project also measured over the less convectively active east Pacific in January - February 2013.

The objective of this paper is to model the transport and distribution of CH_3I, $CHBr_3$ and CH_2Br_2 in the TTL by quantifying their boundary layer and background contribution components using a new Lagrangian methodology. Briefly, the approach quantifies how much of CH_3I, $CHBr_3$ and CH_2Br_2 in the TTL come from the boundary layer, and assesses the role of convection in transporting these compounds to the TTL. The calculation is completed by estimating the background component (i.e. how much of CH_3I, $CHBr_3$ and CH_2Br_2 originate from outside the immediate boundary layer source). Section 2 presents an overview of the field campaigns, the CH_3I, $CHBr_3$ and CH_2Br_2 measurements, and how the NAME calculations are used. In Section 3, the approach is illustrated by comparing model estimates and measurements from one ATTREX 2014 flight. This analysis is then expanded to cover measurements from all ATTREX 2014 and 2013 flights. The role of convection in transporting VSL halocarbons to the TTL is further examined in Section 4. Based on the modelled calculations of $CHBr_3$ and CH_2Br_2, Section 5 discusses how much these VSL bromocarbons contribute to the bromine budget in the TTL.

2 Methodology

2.1 Overview of the CAST, CONTRAST and ATTREX campaigns

The joint CAST, CONTRAST and the third stage of the ATTREX campaign took place in January-March 2014, in the West Pacific. Guam (144.5° E, 13.5° N) was used as a research mission centre for these three campaigns. Three aircraft were deployed to measure physical characteristics and chemical composition of tropical air masses from the earth's surface up to the stratosphere. In CAST, the Facility for Airborne Atmospheric Measurements (FAAM) BAe-146 surveyed the boundary layer and lower troposphere to sample the convection air mass inflow, while in CONTRAST the National Science Foundation - National Center for Atmospheric Research (NSF-NCAR) Gulfstream V (GV) principally target the region of maximum convective outflow in the mid- and upper troposphere and also sampled the boundary layer. Finally, in ATTREX, the NASA Global Hawk (GH) sampled the TTL to cover air masses likely to be detrained from the higher convective outflow. For more details on these campaigns, in particular, objectives, meteorological conditions and descriptions of individual flights, please refer to the campaign summary papers: Harris et al., 2017 (CAST), Pan et al., 2017 (CONTRAST) and Jensen et al., 2017 (ATTREX). ATTREX had four active measurement campaigns, and we also consider the second campaign which was based in Los Angeles in January-March 2013 and which extensively sampled the East and Central Pacific TTL in six research flights.

2.2 Measurements of the VSL halocarbons

Whole Air Samplers (WAS) were deployed on all three aircraft to measure VSL halocarbons. The FAAM BAe-146 and NSF-NCAR GV also used on-board gas chromatography-mass spectrometry

(GC-MS) system for real-time analysis (Wang et al., 2015; Andrews et al., 2016; Pan et al., 2017), though these measurements are not used in our analysis. WAS instrumentation had been used routinely in previous deployments. The sampling and analytical procedures are capable of accessing a wide range of mixing ratios at sufficient precision and the measurements from the three aircraft have been shown to be consistent and comparable (Schauffler et al., 1998; Park et al., 2010; Andrews et al., 2016).

The CAST VSL halocarbon measurements were made using the standard FAAM WAS canisters with 30 second filling time. Up to 64 samples could be collected on each flight and these were analysed in the aircraft hangar, usually within 72 hours after collection. Two litres of sample air were pre-concentrated using a thermal desorption unit (Markes) and analysed with GC-MS (Agilent 7890 GC, 5977 Xtr MSD). Halocarbons were quantified using a NOAA calibration gas standard. The measurement and calibration technique is further described and assessed in Andrews et al. (2013; 2016).

The ATTREX AWAS sampler consisted of 90 canisters, being fully automated and controlled from the ground. Sample collection for the AWAS samples was determined on a real-time basis depending on the flight plan altitude, geographic location, or other relevant real-time measurements. The filling time for each canister ranged from about 25 seconds at 14 km to 90 seconds at 18 km. Canisters were immediately analysed in the field using a high performance GC-MS coupled with a highly sensitive electron capture detector. The limits of detection are compound-dependent and vary from ppt to sub-ppt scale, set at 0.01 ppt for $CHBr_3$, CH_2Br_2 and CH_3I (Navarro et al., 2015). A small artefact of ~0.01-0.02 ppt for CH_3I cannot be excluded. AWAS samples collected on the GV were analysed with the same equipment. Detailed comparison of measurements from the three systems found agreement within ~7 % for $CHBr_3$, ~3 % for CH_2Br_2, and 15 % for CH_3I (Andrews et al., 2016).

2.3 UK Meteorological Office NAME Lagrangian Particle Dispersion Model

The Lagrangian particle dispersion model, NAME, (Jones, et al., 2007) is used to simulate the transport of air masses in the Pacific troposphere and the TTL. Back trajectories are calculated with particles being moved through the model atmosphere by mean wind fields (0.352° longitude and 0.235° latitude, i.e. ~25 km, with 31 vertical levels below 19 km) calculated by the Meteorological Office's Unified Model at 3-hour intervals. This is supplemented by a random walk turbulence scheme (Davies et al., 2005). For this analysis, the NAME model is used with the improved convection scheme, (Meneguz and Thomson, 2014) which simulates displacement of particles subject to convective motions more realistically than previously (Meneguz et al., in review). NAME is run backward in time to determine the origin(s) of air measured at a particular location (WAS sample) along the ATTREX GH flight track.

15,000 particles are released from each point along the flight track where VSL halocarbons were measured in WAS samples. To initialise the NAME model, particles are released randomly in a volume with dimensions 0.1° × 0.1° × 0.3 km centred on each sample. As particles are followed 12

days back in time, trajectories are filtered on the basis of first crossing into the boundary layer (1 km). Subsequently, the fraction of particles which crossed below 1 km is calculated for each WAS measurement point (Ashfold et al., 2012). The NAME 1 km fractions are indicative of the boundary layer air mass influence to the TTL. The 1 km boundary layer fractions are then used to quantitatively estimate the VSL halocarbon contribution to the TTL from the boundary layer, $[X]_{BL\_Contribution}$. In order to compare the measured and modelled halocarbon values, estimates of the contribution from the background troposphere, $[X]_{BG\_Contribution}$ (i.e. air which has not come from the boundary layer within 12 days) are made. The model estimate for the total halocarbon mixing ratio, $[X]_{NAME\_TTL}$, is thus given by Eq. (1):

$$[X]_{NAME_{TTL}} = [X]_{BL\_Contribution} + [X]_{BG\_Contribution} \quad (1)$$

The methods for calculating $[X]_{BL\_Contribution}$ and $[X]_{BG\_Contribution}$ are now described.

2.3.1 NAME modelled boundary layer contribution

The contribution from the boundary layer, ($[X]_{BL\_Contribution}$ - described above) to the VSLs in the TTL can be estimated using

(i) the fractions of trajectories crossing below 1 km in the previous 12 days;
(ii) the transport times to the TTL calculated for each particle;
(iii) the initial concentration values for CH_3I, $CHBr_3$ and CH_2Br_2; and
(iv) their atmospheric lifetimes (to account for the photochemical removal along the trajectory).

More specifically, the boundary layer contribution to the TTL for the VSL halocarbons is calculated using Eq. (2) and Eq. (3):

$$[X]_{BL_{Contribution},t} = [X]_{BL} \times fraction_t \times exp^{(-t/\tau)} \quad (2)$$

$$[X]_{BL\_Contribution} = \sum([X]_{BL_{Contribution},t}) \quad (3)$$

Equation (2) gives the boundary layer contribution to the TTL for a given tracer, X (where X could be CH_3I, $CHBr_3$, CH_2Br_2), at model output time step, t. The model output time step used is 6 hours, from t = 0 (particle release) to t = 48 (end of a 12 day run). $[X]_{BL}$ stands for the initial boundary layer concentration of a given tracer - assigned to each particle which crossed below 1 km (Table 1). $Fraction_t$ is a number of particles which first crossed 1 km in a model output time step, t, over a total number of particles released, and $exp^{(-t/\tau)}$ is a term for the photochemical loss (where τ stands for atmospheric lifetime of a respective VSL halocarbon). Equation (3) gives the boundary layer contribution that is the sum of boundary layer contribution components in all model output time steps (for t = 1 to 48).

Equation (2) calculates the decay of each tracer after it leaves the boundary layer (0-1 km) which is valid for a well-mixed boundary layer. Since 15,000 particles are released for each AWAS sample,

contributions from each particle from below 1 km in the previous 12 days are summed. Decay times, τ, of 4, 15 and 94 days for CH_3I, $CHBr_3$ and CH_2Br_2, respectively, are used (i.e. constant chemical loss rate) (Carpenter et al., 2014). Thus, a particle getting to the TTL in 1 day contributes more of a given tracer to that air mass than a particle taking 10 days. Once this chemical loss term was taken into account, the NAME trajectories can be used to calculate the contribution of convection of air masses from the boundary layer within the preceding 12 days. The initial boundary layer concentrations are derived from the CAST and CONTRAST WAS measurements taken in the West Pacific in the same period of January-March 2014 as for the ATTREX measurements in the TTL (Table 1). These observed means are used in model calculations, and the similarity between them and literature values reported in Carpenter et al. (2014) is seen, with lower values for $CHBr_3$ only.

2.3.2 NAME modelled background contribution

To compare our model results against the AWAS observations, the background contribution, $[X]_{BG\_Contribution}$ (meaning the contribution from the fraction of trajectories which do not cross below 1 km within 12 days) also needs to be accounted for. This requires estimates for the fraction of trajectories from the free troposphere, which is (1-$fraction_{BL}$) , Eq. (4), and an estimate of the halocarbon mixing ratio in that fraction, $[X]_{BG}$, Eq. (5) i.e.

$$fraction_{BL} = \sum(fraction_t) \quad (4)$$

$$[X]_{BG\_Contribution} = (1 - fraction_{BL}) \times [X]_{BG} \quad (5)$$

Since each sample has 15,000 back-trajectories associated with it, some of which came from below 1 km and some of which did not, a definition as to which air samples are considered as boundary layer and which are considered background is required. Two approaches are tested. Both use the NAME calculations to identify AWAS samples in all flights (2013 and 2014) with low convective influence by (i) filtering for air masses with boundary layer fraction values less than 1, 5 or 10 %; and (ii) selecting the lowest 10 % of boundary layer fractions. Then, the CH_3I, $CHBr_3$ and CH_2Br_2 AWAS observations, corresponding to the boundary layer fraction values less than 1, 5 or 10 %, or the lowest 10 % of boundary layer fractions, are averaged to provide CH_3I, $CHBr_3$ and CH_2Br_2 background mixing ratios. Two approaches are explored below (Sect. 3.1.2).

3 Analysis of ATTREX 2014 Research Flight 02

We start by showing our results from one of the individual ATTREX 2014 Research Flights, RF02, to illustrate the method. This is followed by analysing all Research Flights together for ATTREX 2014 and 2013 in Sect. 4, and calculating the modelled contribution of active bromine from very-short lived brominated substances, $CHBr_3$ and CH_2Br_2, to the TTL (Sect. 5).

3.1 Individual ATTREX 2014 Flight: Research Flight 02

Figure 1 shows the vertical distribution of CH_3I, $CHBr_3$ and CH_2Br_2 in the TTL observed during the individual research flight, RF02, during ATTREX 2014. Held on 16-17 February 2014, RF02 was conducted in a confined area east of Guam (12-14° N, 145-147° E) due to a faulty primary satellite communications system for Global Hawk command and control (Jensen, et al., 2017). 26 vertical profiles through TTL were made, with 86 AWAS measurements taken in total. A high degree of variability of CH_3I in the TTL was observed (from > 0.4 ppt at 14-15 km, to near-zero ppt values at 17-18 km). Each profile, in general, showed a gradation in CH_3I distribution in the TTL. Higher values were measured in the lower TTL up to 16 km, with values decreasing with altitude. The same pattern was observed for $CHBr_3$ and CH_2Br_2, with the highest concentrations measured in the lower TTL (14-15 km), and the lowest at 17-18 km.

3.1.1 NAME modelled boundary layer contribution

Figure 2(a) shows the vertical distribution of the boundary layer air contribution to the TTL (corresponding to the AWAS measurement locations along the RF02 flight track). It reveals higher boundary layer air influence in the lower TTL, decreasing with altitude (similarly to the VSL halocarbon observations). Cumulatively, the highest fractions from below 1 km are found for the lower TTL (14-15 km). A noticeable decrease occurs between the lower and upper TTL (15 to 17 km). From 16 km up, little influence (indicated by <10 % and <5 % 1 km fractions of trajectories below 1 km for 16-17 km and 17-18 km, respectively) of the low-level air masses is seen.

Figure 2(b) shows all NAME runs for RF02 grouped into four 1 km TTL bins: 14-15 km, 15-16 km, 16-17 km and 17-18 km. In the 14-15 km bin, most particles from the low troposphere are calculated to have arrived in the preceding 4 days with many in the preceding 2 days. This represents the fast vertical uplift of the low tropospheric air masses to the lower TTL. At 15-16 km, two particle populations are observed: the first group results from recent vertical uplift, while the second group has been in the upper troposphere for longer than a couple of days (see Fig. 2c in Navarro et al., 2015 for similar example). Above 16 km, the overwhelming majority (>90 %) of the released particles are calculated to be in the TTL for the previous 12 days, with negligible evidence for transport from the low troposphere. This shows the dominance of the long-range, horizontal transport for the 16-17 and 17-18 km NAME runs (also shown in Navarro et al., 2015).

Figure 3 shows the locations at which trajectories crossed 1 km, thereby indicating boundary layer source regions for the RF02 TTL air masses. Boundary layer sources in the western and central Pacific are the most important for the lowest TTL bin (14-15 km, Fig. 3a) in this flight. The Maritime Continent, the Northern Australia coast, the Indian Ocean and the equatorial band of the African continent increase in importance as altitude increases, though the overall contribution of recent boundary layer air masses decreases with increasing altitude.

Figure 4 shows the NAME modelled boundary layer contribution to the TTL for CH_3I, $CHBr_3$ and CH_2Br_2 during RF02. It is important to note that this contribution corresponds to uplift from below 1 km in the preceding 12 days, the length of the trajectories. The calculated boundary layer contributions for CH_3I, $CHBr_3$ and CH_2Br_2 from the 1 km fractions are highest at 14-15 km,

dropping off with altitude. Almost no boundary layer contribution is found for 17-18 km (with values close to 0 ppt).

3.1.2 NAME modelled background contribution

Here we explore the two approaches described in Sect. 2.3.2 for estimating the $CHBr_3$ and CH_2Br_2 background mixing ratios. Similar values are seen in ATTREX 2013 and 2014. Less variation is observed for CH_2Br_2 due to its longer atmospheric lifetime.

ATTREX 2013 and 2014 are treated separately in the analysis presented below due to the difference in CH_3I background estimates. The approach using the lowest 10 % of the boundary layer fractions is used to estimate the background contribution for the 2014 flights as not enough data meet the former condition due to the proximity of the flights to strong convection. The background values, inferred from all the ATTREX 2014 flights, are used in the individual flight calculations as again there are not enough data from an individual flight to make background calculations for that flight. In ATTREX 2013 we use the boundary layer fractions less than 5 % approach for the CH_3I background estimation. The ATTREX 2014 background estimates should be taken as upper limits as it is hard to identify samples with no convective influence in 2014. This is especially true for the lower TTL since the ATTREX 2014 flights were close to the region of strong convection.

Figure 5 shows the VSL background mixing ratios calculated for the ATTREX campaigns in 2013 and 2014. In ATTREX 2013, low CH_3I background mixing ratios are found. All approaches show similar background mixing ratios. In 2014, higher CH_3I background mixing ratios are calculated due to ubiquity of air from recent, vertical uplift. No boundary layer fractions less than 1 % are found for the 14-17 km bins, and less than 5 % for the 14-15 km.

3.1.3 NAME modelled total concentrations

The NAME boundary layer and background contribution estimates are added to give an estimate for total halocarbon mixing ratio, $[X]_{NAME\_TTL,}$ (Eq. (1)), for comparison with the AWAS observations.

Figure 6 and Table 2 show the vertical distribution of NAME-based estimates for CH_3I, $CHBr_3$ and CH_2Br_2 in the TTL for RF02. The sums of the NAME CH_3I, $CHBr_3$ and CH_2Br_2 boundary layer and background contribution estimates agree well with the AWAS observations for all the 1 km TTL bins (compared with Fig. 1).

At 14-15 km, the modelled boundary layer contribution of CH_3I is similar to the observations, indicating recent, rapid convective uplift. This provides evidence that the improved convection scheme provides a realistic representation of particle displacement via deep convection. At higher altitudes, the background contribution is more important and, indeed, the modelled total CH_3I values are greater than the observations. This overestimate of the background contribution results from the difficulty of identifying samples with no convective influence in ATTREX 2014. This problem is most important for CH_3I with its very short lifetime.

292 $CHBr_3$ drops off slower with altitude than CH_3I and quicker than CH_2Br_2. At 14-15 km, the boundary
293 layer contribution accounts for ~ 50 % of the modelled sums of $CHBr_3$ and CH_2Br_2, but less than 5 %
294 for $CHBr_3$ and CH_2Br_2 at 17-18 km. For the upper TTL, the background contribution estimates
295 constitute over 85 % of the modelled sums, thus taking on more importance.

296

297 **4 The role of transport in the VSL halocarbon distribution in the TTL**

298 The role of transport in the CH_3I, $CHBr_3$ and CH_2Br_2 distribution in the TTL is examined in this
299 section by applying the NAME based analysis introduced in Sect. 3 to all CH_3I, $CHBr_3$ and CH_2Br_2
300 AWAS observations in the ATTREX 2013 and 2014 campaigns.

301 In ATTREX 2013, six flights surveyed the East Pacific TTL in February-March 2013. Four flights
302 went west from Dryden Flight Research Centre to the area south of Hawaii, reaching 180° longitude.
303 Little influence of convective activity was observed. Most samples with strong boundary layer
304 influence were observed in air masses that had originated over the West Pacific and the Maritime
305 Continent, where it was uplifted to the TTL and transported horizontally within the TTL (Navarro et
306 al., 2015). Two flights sampled the TTL near the Central and South American coast. Few convective
307 episodes were observed. The sampled air had predominantly a small boundary layer air signature
308 from the West Pacific and the Maritime Continent.

309 In ATTREX 2014, two transit flights and six research flights were made in the West Pacific in
310 January-February 2014. This period coincided with the active phase of Madden-Julian Oscillation
311 (MJO) and increased activity of tropical cyclones. A large influence of recent convective events is
312 observed (Navarro et al., 2015), reflected in the elevated CH_3I and $CHBr_3$ mixing ratios and the high
313 values of NAME fractions of trajectories below 1 km. All three aircraft flew together in 2014 and so
314 there is a more complete set of measurements from the ground up. Accordingly, this year is discussed
315 first.

316 **4.1 VSL halocarbon distribution in the TTL: ATTREX 2014**

317 Figure 7 shows the vertical distribution of the observations and of the modelled boundary layer
318 contribution and total mixing ratios for CH_3I, $CHBr_3$ and CH_2Br_2 for all the ATTREX 2014 flights
319 (using only the AWAS measurements made from 20° N southward). As in RF02, CH_3I is highest in
320 the lower TTL, dropping off with altitude. Large flight-to-flight variability in CH_3I measurements is
321 seen. The fraction of NAME particles that travel below 1 km in the previous 12 days (Table 3) are
322 highest at 14-15 km (mean of 57 %) and decrease with altitude in a similar fashion. The CH_3I
323 boundary layer contribution explains most of the observations for the 14-15 and 15-16 km layers.
324 Disparities in observed and modelled CH_3I arise from 16 km up. Background estimate values are
325 minimal, oscillating between 0 and the limit of detection of the AWAS instrument for the iodinated
326 short-lived organic substances, 0.01 ppt. The sums of the CH_3I boundary layer and background

contribution estimates show good agreement with AWAS observations for all the TTL 1 km segments (Table 3).

The good agreement for the 14-15 km and 15-16 km layers can be attributed to the improved representation of deep convection in NAME, provided by the new convection scheme (Meneguz et al., in review). However, there is an underestimation of the boundary layer contribution to the upper TTL levels (16-17 and 17-18 km) which we attribute to the new convection scheme not working as well at these altitudes. Both the CH_3I AWAS observations and the modelled sums are higher than reported previously in the literature (Carpenter et al., 2014) for all the TTL segments. This may be explained by sampling the TTL in a region of high convective activity. This result gives confidence in the quality of the new convection scheme and hence in similar calculations of convective influence on the longer-lived $CHBr_3$ and CH_2Br_2.

The highest $CHBr_3$ and CH_2Br_2 concentrations were observed in the lower TTL (14-15 km), dropping off more slowly with altitude than CH_3I. The weight of the modelled boundary layer contribution estimates to the modelled total amounts varies from approximately 50% at 14-15 km (unlike for CH_3I where over 85 % of the modelled sum is attributed to the boundary layer contribution at 14-15 km) to < 20% at 17-18 km. The sums of the boundary layer and background contribution estimates show good agreement with $CHBr_3$ and CH_2Br_2 AWAS observations. The ATTREX observations and the NAME modelled sums are within the range of values reported in the literature (Carpenter, et al., 2014).

4.2 VSL halocarbon distribution in the TTL: ATTREX 2013

Figure 8 shows the vertical distribution for CH_3I, $CHBr_3$ and CH_2Br_2 in the TTL, observed and modelled from the ATTREX 2013 flights (using only the AWAS measurements taken south of 20°N). Much lower CH_3I values are found in 2013 than in 2014 (Fig. 7). The NAME 1 km fractions are considerably lower (~fourfold), and the corresponding CH_3I boundary layer contribution shows values close to the limit of detection of the AWAS instrument for CH_3I. The background contribution comprises over 85-90 % of the sums of the modelled CH_3I estimate in the TTL. Good agreement is found between the sums of the boundary layer and background contribution estimates, against the AWAS observations. Both the observed and modelled values are in the low end of the CH_3I concentrations reported by the WMO 2014 Ozone Assessment (Carpenter et al., 2014).

The ATTREX 2013 mixing ratios are also lower for $CHBr_3$ and higher CH_2Br_2 than shown in Fig. 7 for 2014. The NAME calculated $CHBr_3$ and CH_2Br_2 boundary layer contributions are small, constituting approximately 10 % of the NAME modelled sums for 14-15 km, and less for the upper TTL segments. The background contribution estimates comprise over 85 % of the modelled sums. Good agreement is found between the sums of the boundary layer and background contribution estimates and the $CHBr_3$ and CH_2Br_2 AWAS observations.

4.3 ATTREX 2013 and 2014: Inter-campaign comparison

Clear differences in the vertical distributions of CH_3I in the TTL are found in ATTREX 2013 and 2014. CH_3I estimates, corresponding to high values in the NAME modelled 1 km fractions, are high in 2014, whereas in 2013 almost no CH_3I is estimated to be in the TTL. This is due to the minimal contribution of the boundary layer air within the previous 12 days: ATTREX 2013 was in the East Pacific away from the main region of strong convection. Longer transport timescales result from horizontal transport and were more important in ATTREX 2013, with much less recent convective influence than in ATTREX 2014. More chemical removal of CH_3I and $CHBr_3$ thus took place, leading to lower concentrations in the East Pacific TTL.

The trajectories are analysed to investigate the timescales for vertical transport by calculating how long it took particles to go from below 1 km to the TTL. In 2013, almost no episodes of recent rapid vertical uplift are found, with most particles taking 8 days and more to cross the 1 km. This is indicative of the dominant role of long-range horizontal transport. In 2014, by way of contrast, a considerable number of trajectories (10's of per cent) come from below 1 km in less than 4 days, representing the 'young' air masses being brought from the low troposphere via recent and rapid vertical uplift.

The spatial variability in the boundary layer air source origins, as well as the variation in atmospheric transport pathways and transport timescales can explain the differences in the distribution of the NAME 1 km fractions in the TTL. In 2014 (2013), higher (lower) boundary layer fractions corresponded well with higher (lower) CH_3I and $CHBr_3$ values in the TTL, especially with the highest concentrations occurring for the flights with the most convective influence and the highest fractions of particles arriving within the 4 days.

In the ATTREX 2014 flights, the western and central Pacific is the dominant source origin of boundary layer air to the TTL (Navarro et al., 2015). Increased tropical cyclone activity in this area (particularly Faxai 28 February – 6 March 2014 and Lusi 7-17 March 2014) and the strong signal from the MJO related convection contributed to the more frequent episodes of strong and rapid vertical uplifts of the low-level air to the TTL. A significant contribution is also seen from the central Indian Ocean, marking the activity of the Fobane tropical cyclone (6-14 February 2014). Minimal contribution from the other remote sources (Indian Ocean, African continental tropical band) is found (Anderson et al., 2016; Jensen et al., 2017; Newton et al., 2018).

5 How much do VSL bromocarbons contribute to the bromine budget in the TTL?

The NAME modelled $CHBr_3$ and CH_2Br_2 estimates in the TTL are used to calculate how much bromine from the VSL bromocarbons, Br-VSL_{org}, is found in the lower stratosphere, based on how much enters the TTL in the form of bromocarbons (as in Navarro et al. (2015)). $CHBr_3$ and CH_2Br_2 are the dominant short-lived organic bromocarbons, and the minor bromocarbons: CH_2BrCl, $CHBr_2Cl$ and $CHBrCl_2$ are excluded here (as their combined contribution is less than 1 ppt to Br-VSL_{org} at 14-18 km, Navarro et al., 2015). The NAME modelled $CHBr_3$ and CH_2Br_2 estimates are multiplied by the number of bromine atoms (bromine atomicity), and then summed to yield the total of Br-VSL_{org}.

Figure 9 shows the contribution of $CHBr_3$ and CH_2Br_2, the two major VSL bromocarbons contributing to the bromine budget in the TTL. For ATTREX 2013 and 2014, similar contributions of $CHBr_3$ and CH_2Br_2 to Br-VSL_{org} are found in the lower TTL. In 2014, $CHBr_3$ in the lower TTL was abundant enough to contribute as much Br-VSL_{org} as CH_2Br_2. A combination of larger boundary layer air influence in the TTL and shorter mean transport times to reach the TTL result in the observed higher $CHBr_3$ contribution to the Br-VSL_{org} in the lower TTL in 2014, than in 2013. The CH_2Br_2 contribution dominates in the upper TTL due to its longer atmospheric lifetime.

Good agreement is found between the bromine loading from the VSL bromocarbons, inferred from the NAME modelled estimates initialised with BAe-146 and GV measurements, and the Global Hawk AWAS observations. Higher organic bromine loading is seen around the cold point tropopause (16-17 km) in ATTREX 2014.

Using the upper troposphere measurements taken during the SHIVA campaign in the western Pacific in November-December 2011, Sala et al. (2014) calculated an estimate for VSLS ($CHBr_3$, CH_2Br_2, $CHBrCl_2$, CH_2BrCl, $CHBr_2Cl$) contribution to the organic bromine at the level of zero radiative heating (15.0 - 15.6 km). Air masses reaching this level are expected to reach the stratosphere. This VSLS mean mixing ratio estimate of 2.88 (+/- 0.29) ppt (2.35 ppt for $CHBr_3$ and CH_2Br_2, excluding minor short-lived bromocarbons) is lower due to a lower contribution from $CHBr_3$ estimate (0.22 ppt compared to $CHBr_3$ estimate for NAME / ATTREX in Table 5). Compared to other literature values reported in Sala et al., (2014), our estimates of the contribution of $CHBr_3$ and CH_2Br_2 to the organic bromine at the LZRH are slightly higher largely due to a higher estimate for a shorter-lived $CHBr_3$.

Navarro et al. (2015) report slightly higher bromine loading from the Br-VSL_{org} at the tropopause level (17 km) in the West Pacific, 2014 than in the East Pacific, 2013 (the Br-VSL_{org} values from the AWAS observations were of 3.27 (+/-0.47) and 2.96 (+/-0.42) ppt, respectively). The minor short-lived organic bromine substances were included in the analysis of Navarro et al. (2015), accounting for the higher Br-VSL_{org}.

Butler et al. (2017), report a mean mole fraction and range of 0.46 (0.13-0.72) ppt and 0.88 (0.71-1.01) ppt of $CHBr_3$ and CH_2Br_2 being transported to the TTL during January and February 2014. This is consistent with a contribution of 3.14 (1.81-4.18) ppt of organic bromine to the TTL over the region of the campaign. The NAME modelled results presented here (Fig. 9, Table 5) are in good agreement with the values reported by Navarro et al. (2015) and Butler et al. (2017).

6 Summary and Discussion

We have used the NAME trajectory model in backward mode to assess the contribution of recent convection to the mixing ratios of three short-lived halocarbons, CH_3I, $CHBr_3$ and CH_2Br_2. 15,000 back-trajectories are computed for each measurement made with the whole air samples on the NASA Global Hawk in ATTREX 2013 and 2014, and the fraction that originated below 1 km is calculated. A steep drop-off in this fraction is observed between 14-15 km and 17-18 km. Low level measurements of CH_3I, $CHBr_3$ and CH_2Br_2 from the FAAM BAe-146 and the NCAR GV are used in

conjunction with these trajectories and an assumed photochemical decay time to provide estimates of the amount of each gas reaching the TTL from below 1 km. Comparison of these modelled estimates with the CH_3I measurements shows good agreement with the observations at the lower altitudes in the TTL values, with less good agreement at altitudes > 16 km, though it should be noted that the amounts are very small here. The lifetime of CH_3I is 3-5 days, and so there is a > 90 % decay in the 12 day trajectories. The comparison between the modelled and measured CH_3I thus indicates that the NAME convection scheme is realistic up to the lower TTL but less good at reproducing the small number of extreme convective events that penetrate to the upper TTL.

In order to perform similar calculations for the longer-lived bromocarbons, an estimate of the background free tropospheric concentration is required. This is calculated by considering bromocarbon values in samples where there was only a small influence from the boundary layer, i.e. where very few NAME trajectories passed below 1 km. This is possible in 2013 when the ATTREX flights were away from the region of strong convection, but much harder in 2014 when (as planned) the flights were heavily influenced by convection. By summing the boundary layer and background contributions, an estimate of the total bromocarbon mixing ratio is obtained.

The resulting modelled estimates are found to be in generally good agreement with the ATTREX measurements. In other words, a high degree of consistency is found between the low altitude halocarbon measurements made on the BAe-146 and GV and the high altitude measurements made on the Global Hawk when they are connected using trajectories calculated by the NAME dispersion model with its updated convection scheme and driven by meteorological analyses with 25 km horizontal resolution.

In the above, the boundary layer contribution arises from trajectories which visit the boundary layer within 12 days while the background contribution involves air that has been transported into the TTL from outside the boundary layer on timescales up to 12 days. Sensitivity tests were performed in which the trajectories were followed for longer than 12 days: the effect was to re-allocate some of the air from the background category into the boundary layer contribution with no net change in the total.

The approach using NAME trajectories and boundary layer measurements produces Br-VSL_{org} estimates of 3.47 +/- 0.4 (3.3 +/- 0.4) ppt in the lower East (West) Pacific TTL (14-15 km) and 2.5 +/-0.2 (2.4 +/-0.4) ppt in the upper East (West) Pacific TTL (17-18 km). These lie well within the range of the recent literature findings (Tegtmeier et al., 2012; Carpenter et al., 2014; Liang et al., 2014; Navarro et al., 2015; Butler et al., 2017). The validation with the ATTREX measurements provides confidence that a similar approach could be used for years when high altitude measurements are not available assuming that realistic estimates of the background tropospheric contributions can be obtained from either models or measurements.

7 Data availability

The CH_3I, $CHBr_3$ and CH_2Br_2 AWAS data from the NASA ATTREX measurements are available online in the NASA ATTREX database (https://espoarchive.nasa.gov/archive/browse/attrex). The CAST measurements are stored on the British Atmospheric Data Centre, which is part of the Centre for Environmental Data archive at http://catalogue.ceda.ac.uk/uuid/565b6bb5a0535b438ad2fae4c852e1b3. The CONTRAST AWAS data are available through http://catalog.eol.ucar.edu/contrast. The NAME data are available from the corresponding author upon request.

8 Author Contribution

The main part of the analysis was conducted by MF. EA and MN provided CH_3I, $CHBr_3$ and CH_2Br_2 AWAS measurements from the ATTREX and CONTRAST research flights. SA and LC provided CH_3I, $CHBr_3$ and CH_2Br_2 measurements from the CAST campaign. MA designed initial scripts for NAME runs and products. EM and DT developed the model code for improved convection scheme. MF and NH prepared the manuscript with contributions from all co-authors, NH also supervised this PhD work.

9 Acknowledgements

The authors would like to thank our NASA ATTREX, NCAR CONTRAST and NERC CAST project partners and the technical teams. MF would like to thank Drs Michelle Cain, Alex Archibald, Sarah Connors, Maria Russo and Paul Griffiths for their input on the NAME applications for flight planning and post-flight modelling. The research was funded through the UK Natural Environment Research Council CAST project (NE/J006246/1 and NE/J00619X/1), and MF was supported by a NERC PhD studentship. EA acknowledges support from NASA grants NNX17AE43G, NNX13AH20G and NNX10AOB3A. We acknowledge use of the NAME atmospheric dispersion model and associated NWP meteorological datasets made available to us by the UK Met Office.

10 References

Anderson, D.C., Nicely, J.M., Salawitch, R.J., Canty, T.P., Dickerson, R.R., Hanisco, T.F., Wolfe, G.M., Apel, E.C., Atlas, E., Bannan, T., Bauguitte, S., Blake, N.J., Bresch, J.F., Campos, T.L., Carpenter, L.J., Cohen, M.D., Evans, M., Fernandez, R.P., Kahn, B.H., Kinnison, D.E., Hall, S.R., Harris, N.R.P.H., Hornbrook, R.S., Lamarque, J-F., Le Breton, M., Lee, J.D., Percival, C., Pfister, L., Bradley Pierce, R., Riemer, D.D., Saiz-Lopez, A., Stunder, B.J.B., Thompson, A.M., Ullmann, K., Vaughan, A., and Weinheimer, A.J.: A pervasive role for biomass burning in tropical high ozone / low water structures, Nature Comms, 7, doi: 10.1038/ncomms10267, 2016.

Andrews, S.J., Jones, C.E., and Carpenter, L.J.: Aircraft measurements of very short-lived halocarbons over the tropical Atlantic Ocean, Geophys Res Lett., 40 (5), 1005-1010, doi: 10.1002/grl.50141, 2013.

508 Andrews, S.J., Carpenter, L.J., Apel, E.C., Atlas, E., Donets, V., Hopkins, J.R., Hornbrook, R.S.,
509 Lewis, A.C., Lidster, R. T., Lueb, R., Minaeian, J., Navarro, M., Punjabi, S., Riemer, D., and
510 Schauffler, S.: A comparison of very short lived halocarbon (VSLS) and DMS aircraft measurements
511 in the tropical west Pacific from CAST, ATTREX and CONTRAST, Atmos. Meas. Tech., 9, 5213-
512 5225, doi: 10.5194/amt-9-5213-2016, 2016.

513 Ashfold, M.J., Harris, N.R.P., Atlas, E.L., Manning, A.J., and Pyle, J.A.: Transport of short-lived
514 species into the Tropical Tropopause Layer, Atmos. Chem. Phys., 12, 6309-6322, doi: 10.5194/acp-
515 12-6309-2012, 2012.

516 Ball, W.T., Alsing, J., Mortlock, D.J., Rozanov, E.V., Tummon, F., and Haigh, J.D.: Reconciling
517 differences in stratospheric ozone composites, Atmos. Chem. Phys., 17, 12269-12302, doi:
518 10.5194/acp-17-12269-2017, 2017.

519 Butler, R., Palmer, P.I., Feng, L., Andrews, S.J., Atlas, E.L., Carpenter, L.J., Donets, V., Harris,
520 N.R.P., Montzka, S.A., Pan, L.L., Salawitch, R.J., and Schauffler, S.M.: Quantifying the vertical
521 transport of $CHBr_3$ and CH_2Br_2 over the Western Pacific, Atmos. Chem. Phys. Discuss., doi:
522 10.5194/acp-2016-936, 2016.

523 Carpenter, L.J., Archer, S.D., and Beale, R.: Ocean-atmosphere trace gas exchange, Chem. Soc.
524 Rev., 41 (19), 6473-6506, doi: 10.1039/c2cs35121h, 2012.

525 Carpenter, L.J., Reimann, S., Burkholder, J.B., Clerbaux, C., Hall, B.D., Hossaini, R., Laube, J.C.,
526 and Yvon-Lewis, S.A.: Ozone-depleting substances (ODSs) and other gases of interest to the
527 Montreal Protocol, Chap.1, in Scientific Assessment of Ozone Depletion, 2014; Global Ozone
528 Research and Monitoring Project – Report no 55, World Meteorological Organisation, Geneva,
529 Switzerland, 2014.

530 Chipperfield, M.P., Bekki, S., Dhomse, S., Harris, N.R.P., Hassler, B., Hossaini, R., Steinbrecht, W.,
531 Thiéblemont, R., and Weber, M.: Detecting recovery of the stratospheric ozone layer, Nature, 549,
532 211–218, doi: 10.1038/nature23681, 2017.

533 Davies, T., Cullen, M.J.P., Malcolm, A.J., Mawson, M.H., Staniforth, A., White, A.A., and Wood,
534 N.: A new dynamical core for the Met Office's global and regional modelling of the atmosphere, Q.
535 J. Roy. Meteorol. Soc., 131, 1759–1782, doi: 10.1256/qj.04.101, 2005.

536 Dessens, O., Zeng, G., Warwick, N., and Pyle, J.: Short-lived bromine compounds in the lower
537 stratosphere; impact of climate change on ozone, Atmos. Sci. Lett., 10, 201-206, doi:
538 10.1002/asl.236, 2009.

539 Fernandez, R.P., Salawitch, R.J., Kinnison, D.E., Lamarque, J-F., and Saiz-Lopez, A.: Bromine
540 partitioning in the tropical tropopause layer: Implications for stratospheric injection, Atmos. Chem.
541 Phys., 14, 13391-13410, doi: 10.5194/acp-14-13391-2014, 2014.

Fiehn, A., Quack, B., Hepach, H., Fuhlbrügge, S., Tegtmeier, S., Toohey, M., Atlas, E., and Krüger, K.: Delivery of halogenated very short-lived substances from the west Indian Ocean to the stratosphere during the Asian summer monsoon, Atmos. Chem. Phys., 17, 6723-6741, doi:10.5194/acp-17-6723-2017, 2017.

Fueglistaler, S., Dessler, A.E., Dunkerton, T.J., Folkins, I., Fu, Q., and Mote, P.W.: Tropical tropopause layer, Reviews of Geophysics, 47 (1), doi:10.1029/2008RG000267, 2009.

Fuhlbrügge, S., Quack, B., Tegtmeier, S., Atlas, E., Hepach, H., Shi, Q., Raimund, S., and Krüger, K.: The contribution of oceanic halocarbons to marine and free tropospheric air over the tropical West Pacific, Atmos. Chem. Phys., 16, 7569-7585, doi:10.5194/acp-16-7569-2016, 2016.

Harris, N.R.P., Hassler, B., Tummon, F., Bodeker, G.E., Hubert, D., Petropavlovskikh, I., Steinbrecht, W., Anderson, J., Bhartia, P.K., Boone, C.D., Bourassa, A., Davis, S.M., Degenstein, D., Delcloo, A., Frith, S.M., Froidevaux, L., Godin-Beekmann, S., Jones, N., Kurylo, M.J., Kyrölä, E., Laine, M., Leblanc, S.T., Lambert, J.-C., Liley, B., Mahieu, E., Maycock, A., de Mazière, M., Parrish, A., Querel, R., Rosenlof, K.H., Roth, C., Sioris, C., Staehelin, J., Stolarski, R.S., Stübi, R., Tamminen, J., Vigouroux, C., Walker, K.A., Wang, H.J., Wild, J., and Zawodny, J.M.: Past changes in the vertical distribution of ozone – Part 3: Analysis and interpretation of trends, Atmos. Chem. Phys., 15, 9965–9982, doi:10.5194/acp- 15-9965-2015, 2015.

Harris, N.R.P., Carpenter, L.J., Lee, J.D., Vaughan, G., Filus, M.T., Jones, R.L., OuYang, B., Pyle, J.A., Robinson, A.D., Andrews, S.J., Lewis, A.C., Minaeian, J., Vaughan, A., Dorsey, J.R., Gallagher, M.W., Le Breton, M., Newton, R., Percival, C.J., Ricketts, H.M.A., Bauguitte, S.J.-B., Nott, G.J., Wellpott, A., Ashfold, M.J., Flemming, J., Butler, R., Palmer, P.I., Kaye, P.H., Stopford, C., Chemel, C., Boesch, H., Humpage, N., Vick, A., MacKenzie, A.R., Hyde, R., Angelov, P., Meneguz, E., and Manning, A.J.: 2017: Coordinated Airborne Studies in the Tropics (CAST), Bull. Amer. Meteor. Soc., 98, 145–162, doi: 10.1175/BAMS-D-14-00290.1, 2017.

Hosking, J.S., Russo, M.R., Braesicke, P. and Pyle, J.A.: Tropical convective transport and the Walker circulation, Atmos. Chem. Phys., 12, 9791-9797, doi: 10.5194/acp-12-9791-2012, 2012.

Hossaini, R., Patra, P.K., Leeson, A.A., Krysztofiak, G., Abraham, N.L., Andrews, S.J., Archibald, A.T., Aschmann, J., Atlas, E.L., Belikov, D.A., Bönisch, H., Carpenter, L.J., Dhomse, S., Dorf, M., Engel, A., Feng, W., Fuhlbrügge, S., Griffiths, P.T., Harris, N.R.P., Hommel, R., Keber, T., Krüger, K., Lennartz, S.T., Maksyutov, S., Mantle, H., Mills, G.P., Miller, B., Montzka, S.A., Moore, F., Navarro, M.A., Oram, D.E., Pfeilsticker, K., Pyle, J.A., Quack, B., Robinson, A.D., Saikawa, E., Saiz-Lopez, A., Sala, S., Sinnhuber, B.-M., Taguchi, S., Tegtmeier, S., Lidster, R.T., Wilson, C., and Ziska, F.: A multi-model intercomparison of halogenated very short-lived substances (TransCom-VSLS): linking oceanic emissions and tropospheric transport for a reconciled estimate of the stratospheric source gas injection of bromine, Atmos. Chem. Phys., 16(14), 9163-9187, doi:10.5194/acp-16-9163-2016, 2016.

578 Hossaini, R., Chipperfield, M., Montzka, S.A., Leeson, A.A., Dhomse, S.S., and Pyle, J.A.: The
579 increasing threat to stratospheric ozone from dichloromethane, Nature Comms., doi:
580 10.1038/ncomms15962, 2017.

581 Jensen, E.J., Pfister, L., Jordan, D.E., Bui, T.V., Ueyama, R., Singh, H.B., Thornberry, T.D., Rollins,
582 A.W., Gao, R., Fahey, D.W., Rosenlof, K.H., Elkins, J.W., Diskin, G.S., DiGangi, J.P., Lawson,
583 R.P., Woods, S., Atlas, E.L., Navarro Rodriguez, M.A., Wofsy, S.C., Pittman, J., Bardeen, C.G.,
584 Toon, O.B., Kindel, B.C., Newman, P.A., McGill, M.J., Hlavka, D.L., Lait, L.R., Schoeberl, M.R.,
585 Bergman, J.W., Selkirk, H.B., Alexander, M.J., Kim, J.-E., Lim, B.H., Stutz, J., and Pfeilsticker, K.:
586 The NASA Airborne Tropical Tropopause Experiment: High-Altitude Aircraft Measurements in the
587 Tropical Western Pacific, Bull. Amer. Meteor. Soc., 98, 129–143, doi:10.1175/BAMS-D-14-
588 00263.1, 2017.

589 Jones, A., Thomson, D., Hort, M., and Devenish, B.: The U.K. Met Office's Next-Generation
590 Atmospheric Dispersion Model, NAME III Air Pollution Modeling and Its Application XVII,
591 Springer US, 580-589, doi: 10.1007/978-0-387-68854-1_62, 2007.

592 Krzysztofiak, G., Catoire, V., Hamer, P.D., Marécal, V., Robert, C., Engel, A., Bönisch, H.,
593 Grossman, K., Quack, B., Atlas, E. and Pfeilsticker, K.: Evidence of convective transport in tropical
594 West Pacific region during SHIVA experiment, Atmos. Sci. Lett., 19, 1-7, doi: 10.1002/asl.798,
595 2018.

596 Liang, Q., Stolarski, R.S., Kawa, S.R., Nielsen, J.E., Douglass, A.R., Rodriguez, J.M., Blake, D.R.,
597 Atlas, E.L., and Ott, L.E.: Finding the missing stratospheric Bry: a global modelling study of $CHBr_3$
598 and CH_2Br_2, Atmos. Chem. Phys., 10, 2269-2286, doi: 10.5194/acp-10-2269-2010, 2010.

599 Liang, Q., Atlas, E., Blake, D., Dorf, M., Pfeilsticker, K. and Schauffler, S.: Convective transport of
600 very short-lived bromocarbons to the stratosphere, Atmos. Chem. Phys. Discuss., 14, 651-676, doi:
601 10.5194/acpd-14-651-2014, 2014.

602 Lovelock, J.E.: Natural halocarbons in the air and in the sea, Nature, 256, 193-194, doi:
603 10.1038/256193a0, 1975.

604 Meneguz, E. and Thomson, D.J.: Towards a new scheme for parametrization of deep convection in
605 NAME III, Int. J. Environ. Pollut., 54, 128-136, doi: 10.1504/IJEP.2014.065113, 2014.

606 Meneguz, E., Thomson, D.J., Witham, C., Filus, M.T., Harris, N.R.P., Navarro, M. and Atlas, E.:
607 Improved parameterisation scheme to represent tropospheric moist convection in NAME, (in
608 review).

609 Navarro, M.A., Atlas, E.A., Saiz-Lopez, A., Rodriguez-Lloveras, X., Kinnison, D.E., Lamarque, J.-
610 F., Tilmes, S., Filus, M., Harris, N.R.P., Meneguz, E., Ashfold, M.J., Manning, A.J., Cuevas, C.A.,
611 Schauffler, S.M., and Donets, V.: Airborne measurements of organic bromine compounds in the

612 Pacific tropical tropopause layer, PNAS., USA, 112, 13789-13793, doi: 10.1073/pnas.1511463112,
613 2015.
614
615 Newton, R., Vaughan, G., Hintsa, E., Filus, M.T., Pan, L.L., Honomichl, S., Atlas, E., Andrews, S.J.,
616 and Carpenter, L.J.: Observations of ozone-poor air in the tropical tropopause layer, Atmos. Chem.
617 Phys., 18, 5157-5171, doi:10.5194/acp-18-5157-2018, 2018.
618
619 Oram, D.E. and Penkett, S.A.: Observations in eastern England of elevated methyl iodide
620 concentrations in air of Atlantic origin, Atmos. Environ., 28, 1159-1174, doi: 10.1016/1352-
621 2130(94)90293-3, 1994.
622
623 Oram, D.E., Ashfold, M.J., Laube, J.C., Gooch, L.J., Humphrey, S., Sturges, W.T., Leedham-
624 Elvidge, E., Forster, G.L., Harris, N.R.P., Mead, M.I., Samah, A.A., Phang, S.M., Ou-Yang, C.-F.,
625 Lin, N.-H., Wang, J.-L., Baker, A.K., Brenninkmeijer, C.A.M., and Sherry, D.: A growing threat to
626 the ozone layer from short-lived anthropogenic chlorocarbons, Atmos. Chem. Phys., 17, 11929-
627 11941, doi: 10.5194/acp-17-11929-2017, 2017.

628 Pan, L.L., Atlas, E.L., Salawitch, R.J., Honomichl, S.B., Bresch, J.F., Randel, W.J., Apel, E.C.,
629 Hornbrook, R.S., Weinheimer, A.J., Anderson, D.C., Andrews, S.J., Baidar, S., Beaton, S.P.,
630 Campos, T.L., Carpenter, L.J., Chen, D., Dix, B., Donets, V., Hall, S.R., Hanisco, T.F., Homeyer,
631 C.R., Huey, L.G., Jensen, J.B., Kaser, L., Kinnison, D.E., Koenig, T.K., Lamarque, J., Liu, C., Luo,
632 J., Luo, Z.J., Montzka, D.D., Nicely, J.M., Pierce, R.B., Riemer, D.D., Robinson, T., Romashkin, P.,
633 Saiz-Lopez, A., Schauffler, S., Shieh, O., Stell, M.H., Ullmann, K., Vaughan, G., Volkamer, R., and
634 Wolfe, G.: The Convective Transport of Active Species in the Tropics (CONTRAST) Experiment,
635 Bull. Amer. Meteor. Soc., 98, 106–128, doi:10.1175/BAMS-D-14-00272.1, 2017.

636 Park, S., Atlas, E.L., Jiménez, R., Daube, B.C., Gottlieb, E.W., Nan, J., Jones, D.B.A., Pfister, L.,
637 Conway, T.J., Bui, T.P., Gao, R.-S., and Wofsy, S.C.: Vertical transport rates and concentrations of
638 OH and Cl radicals in the Tropical Tropopause Layer from observations of CO_2 and halocarbons:
639 implications for distributions of long- and short-lived chemical species, Atmos. Chem. Phys., 10,
640 6669-6684, doi: 10.5194/acp-10-6669-2010, 2014.

641 Pfeilsticker, K., Sturges, W.T., Bosch, H., Camy-Peyret, C., Chipperfield, M.P., Engel, A.,
642 Fitzenberger, R., Muller, M., Payan, S., and Sinnhuber, B.-M.: Lower stratospheric organic and
643 inorganic bromine budget for the arctic winter 1998/1999, Geophys. Res. Lett., 27, 3305-3308, doi:
644 10.1029/2000GL011650, 2000.

645 Pyle, J.A., Ashfold, M.J., Harris, N.R.P., Robinson, A.D., Warwick, N.J., Carver, G.D., Gostlow, B.,
646 O'Brien, L.M., Manning, A.J., Phang, S.M., Yong, S.E., Leong, K.P., Ung, E.H., and Ong, S.:
647 Bromoform in the tropical boundary layer of the Maritime Continent during OP3, Atmos. Chem.
648 Phys., 11, 529-542, doi: 10.5194/acp-11-529-2011, 2011.

649 Russo, M.R., Marécal, V., Hoyle, C.R., Arteta, J., Chemel, C., Chipperfield, M.P., Dessens, O.,
650 Feng, W., Hosking, J.S., Telford, P.J., Wild, O., Yang, X., and Pyle, J.A.:Representation of deep
651 convection in atmospheric models – Part 1: Meteorology and comparison with satellite observations,
652 Atmos. Chem. Phys., 11, 2765-2786, doi: 10.5194/acp-11-2765-2011, 2011.

653 Russo, M.R., Ashfold, M.J., Harris, N.R.P., and Pyle, J.A.: On the emissions and transport of
654 bromoform: sensitivity to model resolution and emission location, Atmos. Chem. Phys., 15, 14031-
655 14040, doi: 10.5194/acp-15-14031-2015, 2015.

656 Saiz-Lopez, A., Fernandez, R.P., Ordóñez, C., Kinnison, D.E., Gómez-Martin, J.C., Lamarque, J.-F.,
657 and Tilmes, S.: Iodine chemistry in the troposphere and its effects on ozone, Atmos. Chem. Phys.,
658 14, 13119-13143, doi: 10.5194/acp-14-13119-2014, 2014.

659 Sala, S., Bönisch, H., Keber, T., Oram, D.E., Mills, G., and Engel, A.: Deriving an atmospheric
660 budget of total organic bromine using airborne in situ measurements from western Pacific area
661 during SHIVA, Atmos. Chem. Phys., 14, 6903-6923, doi:10.5194/acp-14-6903-2014, 2014.

662 Schauffler, S.M., Atlas, E.L., Flocke, F., Lueb, R.A., Stroud, V., and Travnicek, W.: Measurements
663 of bromine containing organic compounds at the tropical tropopause, Geophys. Res.Lett., 25, 3,317-
664 320, doi:10.1029/98GL00040, 1998.

665 Schofield, R., Fueglistaler, S., Wohltmann, I., and Rex, M.: Sensitivity of stratospheric Bry to
666 uncertainties in very short lived substance emissions and atmospheric transport, Atmos. Chem. Phys.,
667 11, 1379–1392, doi:10.5194/acp-11-1379-2011, 2011.

668 Solomon, S., Garcia, R.R., and Ravishankara, A.R.: On the role of iodine in ozone depletion, J.
669 Geophys. Res., 99, 20941, doi: 10.1029/94JD02028, 1994.

670 Steinbrecht, W., Froidevaux, L., Fuller, R., Wang, R., Anderson, J., Roth, C., Bourassa, A.,
671 Degenstein, D., Damadeo, R., Zawodny, J., Frith, S., McPeters, R., Bhartia, P., Wild, J., Long, C.,
672 Davis, S., Rosenlof, K., Sofieva, V., Walker, K., Rahpoe, N., Rozanov, A., Weber, M., Laeng, A.,
673 von Clarmann, T., Stiller, G., Kramarova, N., Godin-Beekmann, S., Leblanc, T., Querel, R., Swart,
674 D., Boyd, I., Hocke, K., Kämpfer, N., Maillard Barras, E., Moreira, L., Nedoluha, G., Vigouroux, C.,
675 Blumenstock, T., Schneider, M., García, O., Jones, N., Mahieu, E., Smale, D., Kotkamp, M.,
676 Robinson, J., Petropavlovskikh, I., Harris, N., Hassler, B., Hubert, D., and Tummon, F.: An update
677 on ozone profile trends for the period 2000 to 2016, Atmos. Chem. Phys., 17, 10675– 10690, doi:
678 10.5194/acp-17-10675-2017, 2017.

679 Tegtmeier, S., Krüuger, K., Quack, B., Atlas, E.L., Pisso, I., Stohl, A., and Yang, X.: Emission and
680 transport of bromocarbons: from the West Pacific ocean into the stratosphere, Atmos. Chem. Phys.,
681 12, 10633-10648, doi: 10.5194/acp-12-10633-2012, 2012.

Tegtmeier, S., Krüger, K., Quack, B., Atlas, E., Blake, D.R., Boenish, H., Engel, A., Hepach, H., Hossaini, R., Navarro, M.A., Raimund, S., Sala, S., Shi, Q., and Ziska, F.: The contribution of oceanic methyl iodide to stratospheric iodine, Atmos. Chem. Phys., 13, 11869-11886, doi: 10.5194/acp-13-11869-2013, 2013.

Tegtmeier, S., Ziska, F., Pisso, I., Quack, B., Velders, G.J.M., Yang, X., and Krüger, K.: Oceanic bromoform emissions weighted by their ozone depletion potential, Atmos. Chem. Phys., 15, 13647-13663, doi: 10.5194/acp-15-13647-2015, 2015.

Vogt, R., Sander, R., von Glasow, R. and Crutzen, P.J.: Iodine chemistry and its role in halogen activation and ozone loss in the marine boundary layer: a model study, J. Atmos. Chem., 32, 375-395, doi: 10.1023/A:1006179901037, 1999.

Wang, S., Schmidt, J.A., Baidar, S., Coburn, S., Dix, B., Koenig, T.K., Apel, E., Bowdalo, D., Campos, T.L., Eloranta, E., Evans, M.J., DiGangi, J.P., Zondlo, M.A., Gao, R.S., Haggerty, J.A., Hall, S.R., Hornbrook, R.S., Jacob, D., Morley, B., Pierce, B., Reeves, M., Romashkin, P., Ter Schure A., and Volkamer, R.:Active and widespread halogen chemistry in the tropical and subtropical free troposphere, PNAS, 112 (30), 9281-9286, doi:10.1073/pnas.1505142112, 2015.

11 Tables

Table 1. Boundary layer concentrations and atmospheric lifetimes for CH_3I, $CHBr_3$ and CH_2Br_2 (Carpenter et.al., 2014).

Tracer, [X]	**Boundary Layer Concentration, $[X]_{BL}$ [ppt]**		**Atmospheric Lifetime, τ [days]**
	CAST and CONTRAST Mean (Range) Median	Carpenter et al., 2014 Median (Range)	
CH_3I	0.70 (0.16-3.34) 0.65	0.8 (0.3-2.1)	4
$CHBr_3$	0.83 (0.41-2.56) 0.73	1.6 (0.5-2.4)	15
CH_2Br_2	0.90 (0.61-1.38) 0.86	1.1 (0.7-1.5)	94

Atmos. Chem. Phys. Discuss., https://doi.org/10.5194/acp-2018-640
Manuscript under review for journal Atmos. Chem. Phys.
Discussion started: 7 September 2018

Atmospheric Chemistry and Physics Discussions

704

705 *Table 2. ATTREX 2014 Research Flight 02: AWAS observations, modelled boundary layer*
706 *contribution, the modelled total mixing ratios for CH_3I, $CHBr_3$ and CH_2Br_2. The boundary layer and*
707 *background fractions means and standard deviations (in brackets) are given based on the*
708 *measurements and modelled values for the samples collected during the flight.*

Altitude [km]	**AWAS [ppt]**	**Modelled Boundary Layer Contribution [ppt]**	**Modelled Total Mixing Ratio [ppt]**
CH_3I			
17-18	0.06 (0.02)	0.00 (0.00)	0.06 (0.02)
16-17	0.09 (0.03)	0.00 (0.00)	0.06 (0.02)
15-16	0.17 (0.03)	0.04 (0.04)	0.12 (0.06)
14-15	0.23 (0.09)	0.17 (0.04)	0.21 (0.08)
$CHBr_3$			
17-18	0.34 (0.17)	0.01 (0.00)	0.29 (0.15)
16-17	0.42 (0.11)	0.03 (0.01)	0.36 (0.14)
15-16	0.55 (0.06)	0.12 (0.07)	0.48 (0.17)
14-15	0.67 (0.10)	0.35 (0.07)	0.58 (0.13)
CH_2Br_2			
17-18	0.72 (0.02)	0.02 (0.01)	0.71 (0.03)
16-17	0.79 (0.07)	0.06 (0.02)	0.76 (0.06)
15-16	0.83 (0.05)	0.19 (0.09)	0.78 (0.10)
14-15	0.89 (0.05)	0.46 (0.08)	0.84 (0.12)

	Boundary Layer fraction [%]	***Background fraction [%]***
17-18	2.1 (1.1)	97.9
16-17	7.2 (2.7)	92.8
15-16	22.9 (10.0)	77.1
14-15	53.3 (9.0)	46.7

709

Atmos. Chem. Phys. Discuss., https://doi.org/10.5194/acp-2018-640
Manuscript under review for journal Atmos. Chem. Phys.
Discussion started: 7 September 2018

Atmospheric Chemistry and Physics Discussions

710

711 *Table 3. ATTREX 2014 all flights: AWAS observations, modelled boundary layer contribution, the*
712 *modelled total mixing ratios for CH_3I, $CHBr_3$ and CH_2Br_2. The boundary layer and background*
713 *fractions are also given. Means and standard deviations (in brackets).*

Altitude [km]	**AWAS [ppt]**	**Modelled Boundary Layer Contribution [ppt]**	**Modelled Total Mixing Ratio [ppt]**
CH_3I			
17-18	0.04 (0.03)	0.02 (0.03)	0.07 (0.04)
16-17	0.11 (0.10)	0.04 (0.04)	0.09 (0.05)
15-16	0.16 (0.14)	0.09 (0.07)	0.15 (0.08)
14-15	0.17 (0.14)	0.15 (0.08)	0.19 (0.11)
$CHBr_3$			
17-18	0.33 (0.14)	0.06 (0.06)	0.32 (0.16)
16-17	0.48 (0.13)	0.12 (0.09)	0.40 (0.17)
15-16	0.54 (0.13)	0.21 (0.12)	0.50 (0.19)
14-15	0.61 (0.13)	0.31 (0.12)	0.55 (0.16)
CH_2Br_2			
17-18	0.73 (0.06)	0.11 (0.09)	0.73 (0.09)
16-17	0.82 (0.08)	0.19 (0.14)	0.78 (0.15)
15-16	0.84 (0.09)	0.32 (0.16)	0.80 (0.17)
14-15	0.86 (0.07)	0.44 (0.15)	0.84 (0.17)

	Boundary Layer fraction [%]	***Background fraction [%]***
17-18	12.7 (10.9)	87.3
16-17	22.3 (16.0)	77.7
15-16	37.8 (18.8)	62.2
14-15	51.7 (16.1)	48.3

714

715

716

Atmos. Chem. Phys. Discuss., https://doi.org/10.5194/acp-2018-640
Manuscript under review for journal Atmos. Chem. Phys.
Discussion started: 7 September 2018

Atmospheric Chemistry and Physics Discussions

Table 4. ATTREX 2013 all flights: AWAS observations, modelled boundary layer contribution, the modelled total mixing ratios for CH_3I, $CHBr_3$ and CH_2Br_2. The boundary layer and background fractions are also given. Means and standard deviations (in brackets).

Altitude [km]	**AWAS [ppt]**	**Modelled Boundary Layer Contribution [ppt]**	**Modelled Total Mixing Ratio [ppt]**
CH_3I			
17-18	0.03 (0.02)	0.00 (0.00)	0.03 (0.01)
16-17	0.03 (0.02)	0.00 (0.00)	0.03 (0.02)
15-16	0.04 (0.02)	0.01 (0.01)	0.03 (0.03)
14-15	0.04 (0.03)	0.01 (0.01)	0.05 (0.03)
$CHBr_3$			
17-18	0.31 (0.10)	0.01 (0.01)	0.31 (0.09)
16-17	0.39 (0.12)	0.02 (0.02)	0.35 (0.11)
15-16	0.54 (0.15)	0.04 (0.04)	0.49 (0.16)
14-15	0.53 (0.15)	0.07 (0.05)	0.53 (0.18)
CH_2Br_2			
17-18	0.79 (0.08)	0.02 (0.04)	0.78 (0.07)
16-17	0.83 (0.07)	0.04 (0.04)	0.81 (0.07)
15-16	0.90 (0.07)	0.07 (0.06)	0.87 (0.10)
14-15	0.91 (0.08)	0.12 (0.09)	0.89 (0.12)

	Boundary Layer fraction [%]	***Background fraction [%]***
17-18	1.9 (2.3)	98.1
16-17	4.7 (4.9)	95.3
15-16	9.8 (7.9)	90.2
14-15	14.7 (11.1)	85.3

Atmos. Chem. Phys. Discuss., https://doi.org/10.5194/acp-2018-640
Manuscript under review for journal Atmos. Chem. Phys.
Discussion started: 7 September 2018

Atmospheric Chemistry and Physics Discussions

721

722

723

724 *Table 5. Contribution from the very short-lived bromocarbons: $CHBr_3$ and CH_2Br_2 to the bromine in*
725 *the TTL as given by modelled estimates and AWAS observations for ATTREX 2014 and 2013.*
726 *[$CHBr_3$] and [CH_2Br_2] means are shown only.*

Altitude [km]	**[$CHBr_3$] [ppt]**	**[CH_2Br_2] [ppt]**	**Br from $CHBr_3$ [ppt]**	**Br from CH_2Br_2 [ppt]**	**Br-VSL_{org} [ppt]**
ATTREX 2014					
NAME					
17-18	0.32	0.73	0.96	1.46	2.42
16-17	0.40	0.78	1.20	1.56	2.76
15-16	0.50	0.80	1.50	1.60	3.10
14-15	0.55	0.84	1.65	1.68	3.33
AWAS					
17-18	0.33	0.73	0.99	1.46	2.45
16-17	0.48	0.82	1.44	1.64	3.08
15-16	0.54	0.84	1.62	1.68	3.30
14-15	0.61	0.86	1.83	1.72	3.55
ATTREX 2013					
NAME					
17-18	0.31	0.78	0.93	1.56	2.49
16-17	0.35	0.81	1.05	1.62	2.67
15-16	0.49	0.87	1.47	1.74	3.21
14-15	0.53	0.89	1.59	1.78	3.37
AWAS					
17-18	0.31	0.79	0.93	1.58	2.51
16-17	0.39	0.83	1.17	1.66	2.83
15-16	0.54	0.90	1.62	1.80	3.42
14-15	0.53	0.91	1.59	1.82	3.41

727

Atmos. Chem. Phys. Discuss., https://doi.org/10.5194/acp-2018-640
Manuscript under review for journal Atmos. Chem. Phys.
Discussion started: 7 September 2018

728 **12 Figures**

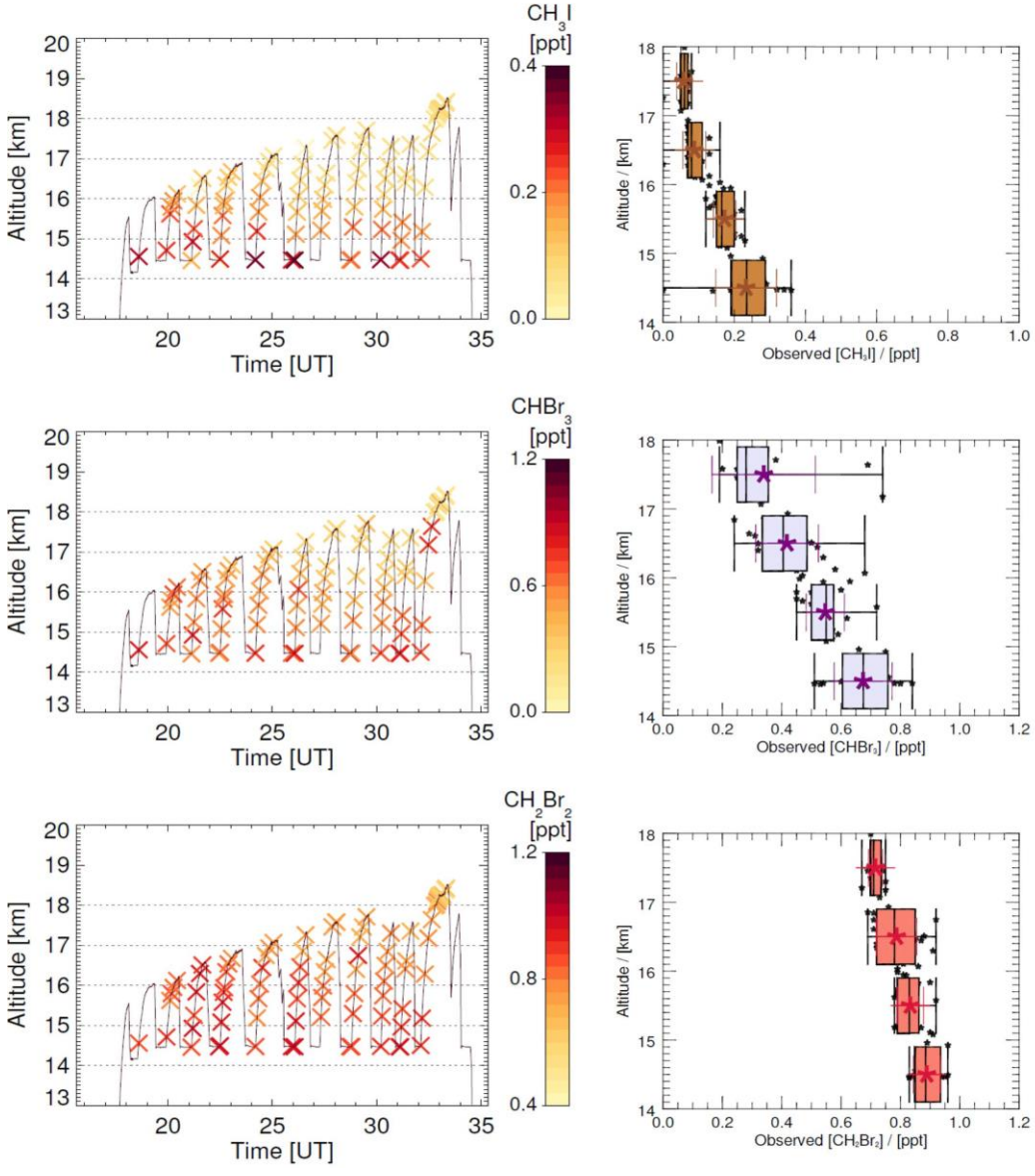

729

730 **Figure 1:** Vertical distribution of CH_3I, $CHBr_3$ and CH_2Br_2 in the TTL, as measured during Research
731 Flight 02, ATTREX 2014: AWAS measurements along the flight track (left), observations grouped
732 into 1 km TTL segments (right, means (star symbols), standard deviations (coloured whiskers),
733 minimum, lower and upper quartiles, median and maximum (black box and whiskers)).

Atmos. Chem. Phys. Discuss., https://doi.org/10.5194/acp-2018-640
Manuscript under review for journal Atmos. Chem. Phys.
Discussion started: 7 September 2018

Atmospheric Chemistry and Physics Discussions

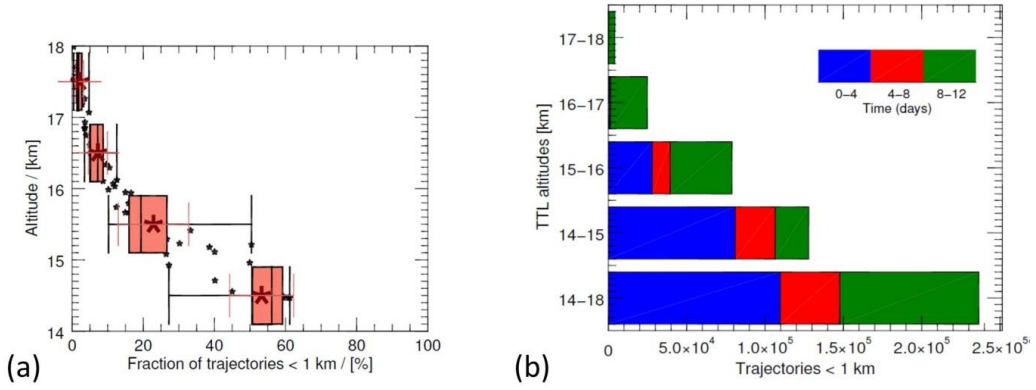

734

735 **Figure 2:** Vertical distribution of NAME 1 km fractions (the fractions which reach the boundary
736 layer within 12 days - indicative of boundary layer air influence) in the TTL (2a, left). Distribution of
737 transport times taken for the trajectories to first cross below 1 km (reach boundary layer) for all the
738 NAME runs and the NAME runs grouped into 1 km TTL segments, Research Flight 02, ATTREX
739 2014 (2b, right).

740

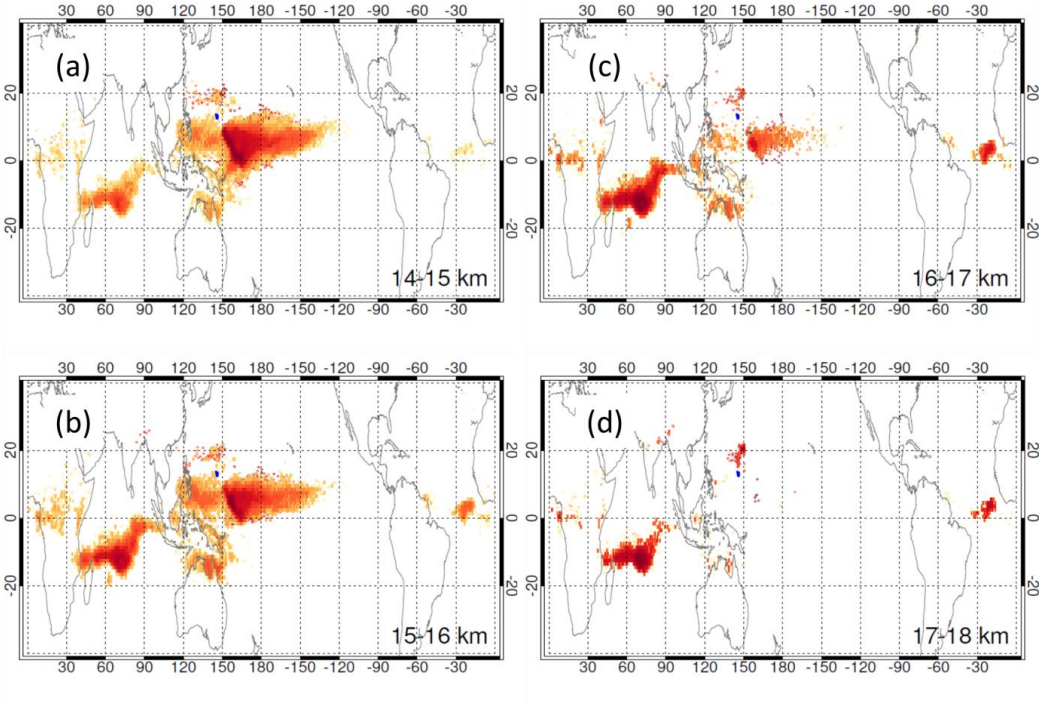

741

Atmos. Chem. Phys. Discuss., https://doi.org/10.5194/acp-2018-640
Manuscript under review for journal Atmos. Chem. Phys.
Discussion started: 7 September 2018

Atmospheric Chemistry and Physics Discussions

742 **Figure 3:** Crossing location distribution maps for all the NAME runs released from 4 1 km TTL
743 altitudes: 14-18 km. Strong influence of local boundary air is noted for a 14-15 km segment (lower
744 TTL), whereas the boundary air from remote locations dominates for a 17-18 km segment (upper
745 TTL), Research Flight 02, ATTREX 2014.

746

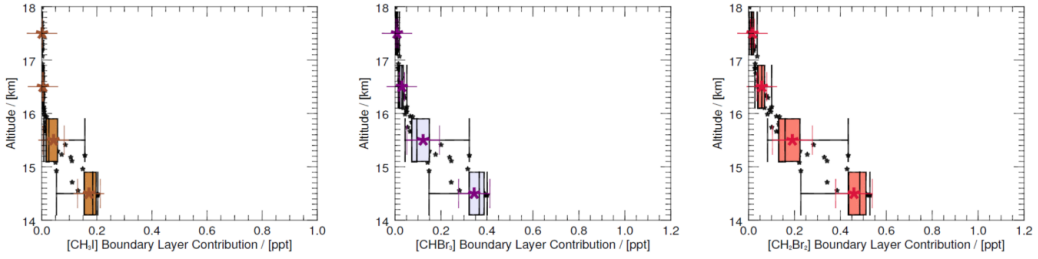

747

748 **Figure 4:** NAME modelled CH_3I, $CHBr_3$ and CH_2Br_2 boundary layer contribution to the TTL,
749 Research Flight 02, ATTREX 2014.

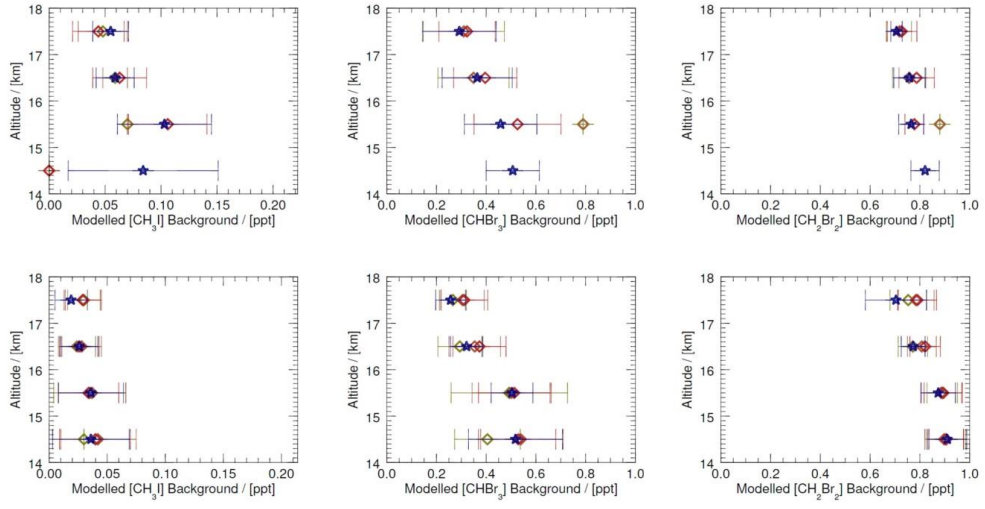

750

751 **Figure 5:** Background mixing ratios for CH_3I, $CHBr_3$ and CH_2Br_2 for all NAME runs for all flights
752 in ATTREX 2014 (top row) and ATTREX 2013 (bottom row). Little convective influence is
753 indicated by selecting means from NAME 1 km fractions of <1 (blue star), 5 (red diamond) and 10
754 (green diamond) %.

Atmos. Chem. Phys. Discuss., https://doi.org/10.5194/acp-2018-640
Manuscript under review for journal Atmos. Chem. Phys.
Discussion started: 7 September 2018

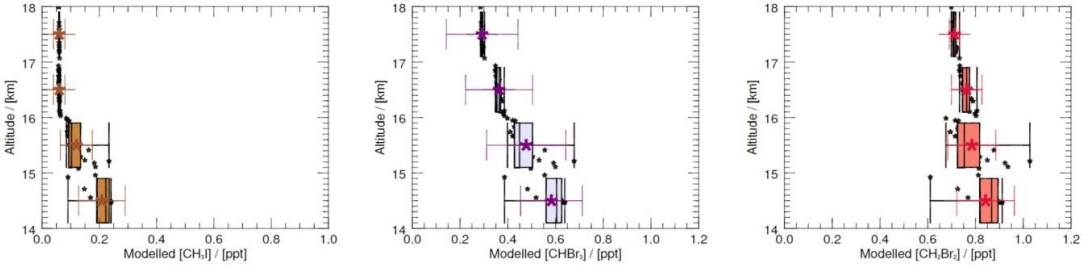

Figure 6: Vertical distribution of NAME modelled CH_3I, $CHBr_3$ and CH_2Br_2 (sums of boundary layer and background contribution) in the TTL for Research Flight 02, ATTREX 2014.

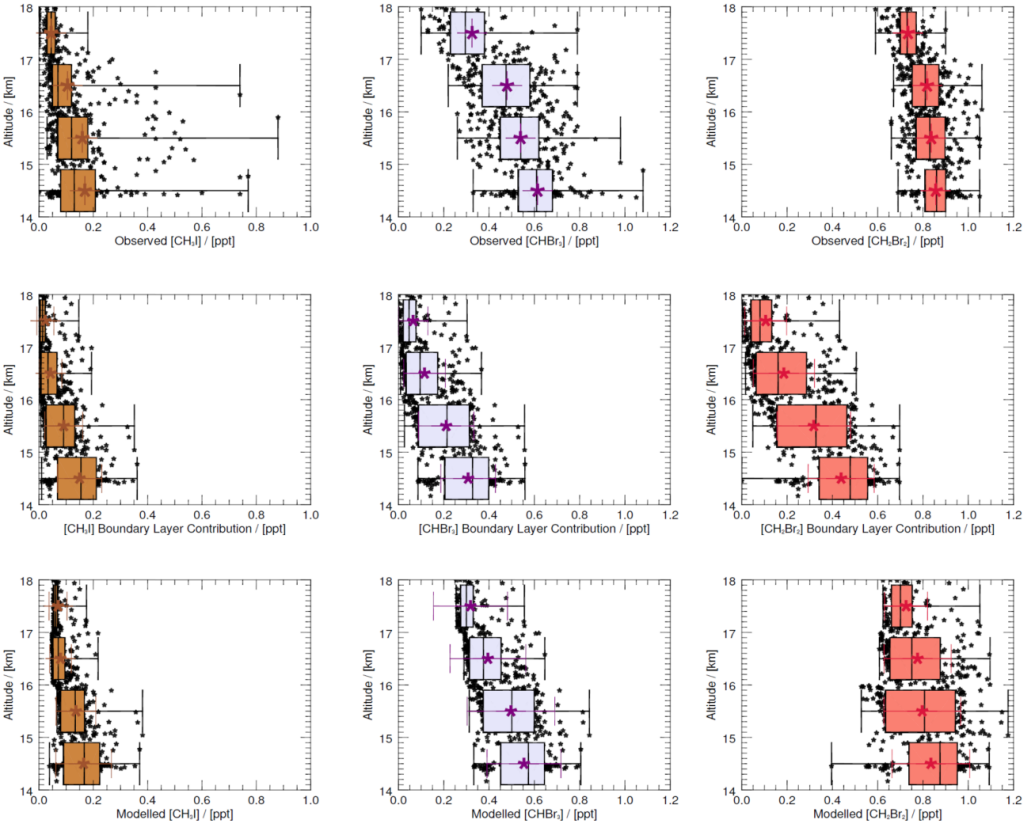

Atmos. Chem. Phys. Discuss., https://doi.org/10.5194/acp-2018-640
Manuscript under review for journal Atmos. Chem. Phys.
Discussion started: 7 September 2018

Atmospheric Chemistry and Physics Discussions

760 **Figure 7:** CH_3I, $CHBr_3$ and CH_2Br_2 vertical distribution in the TTL for ATTREX 2014 flights:
761 AWAS observations (top row), NAME modelled boundary layer contribution (middle row), and
762 NAME modelled sums of boundary layer and background contributions (bottom row).

763

764

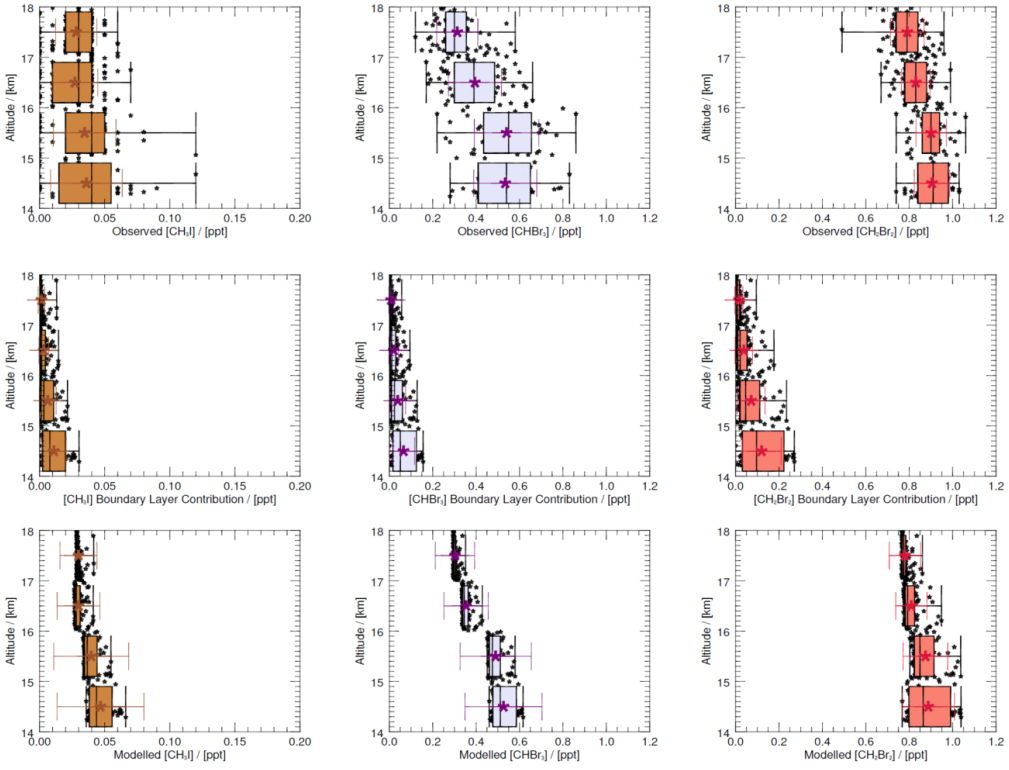

765

766 **Figure 8:** CH_3I, $CHBr_3$ and CH_2Br_2 vertical distribution in the TTL for ATTREX 2013 flights:
767 AWAS observations (top row), NAME modelled boundary layer contribution (middle row), and
768 NAME modelled sums of boundary layer and background contributions (bottom row).

Atmos. Chem. Phys. Discuss., https://doi.org/10.5194/acp-2018-640
Manuscript under review for journal Atmos. Chem. Phys.
Discussion started: 7 September 2018

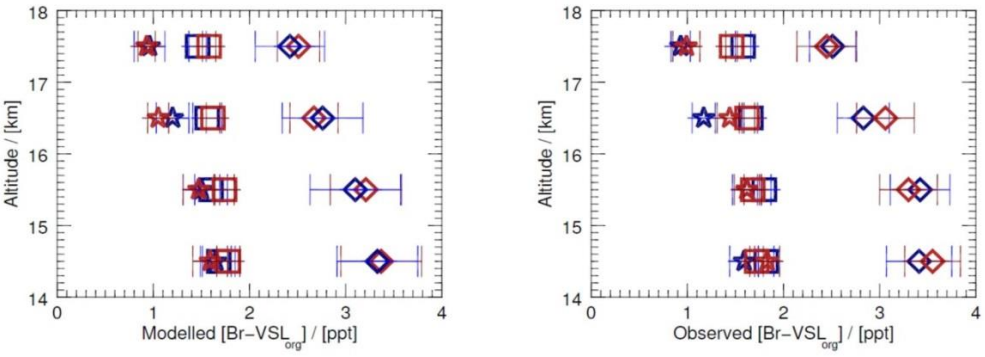

769

770 **Figure 9:** Contribution of $CHBr_3$ (star symbol) and CH_2Br_2 (square symbol) to the bromine budget in
771 the TTL, inferred from the NAME modelled estimates (left) and AWAS observations (right);
772 separately ATTREX 2014 (red) and 2013 (blue). Star and square symbols represent the bromine
773 atomicity products from $CHBr_3$ and CH_2Br_2, respectively. Diamonds show the bromine contribution
774 from the VSL bromocarbons in the TTL (as a sum of the $CHBr_3$ and CH_2Br_2 bromine atomicity
775 products).

776